Microstructure and mechanical properties of thermomechanically processed TRIP steel

I.B. Timokhina, P.D. Hodgson, H. Beladi, E.V. Pereloma

The strengthening mechanism responsible for the unique combination of ultimate tensile strength and elongation in a multiphase Fe-0.2C-1.5Mn-1.2Si-0.3Mo-0.6Al-0.02Nb (wt%) steel was studied. The microstructures with different volume fractions of polygonal ferrite, bainite and retained austenite were simulated by controlled thermomechanical processing. The interrupted tensile test was used to study the bainitic ferrite, retained austenite and polygonal ferrite behaviour as a function of plastic strain. X-ray analysis was used to characterise the volume fraction and carbon content of retained austenite. Transmission electron microscopy was utilised to analyse the effect of bainitic ferrite morphology on the strain induced transformation of retained austenite and retained austenite twinning as a function of strain in the bulk material. The study has shown that the austenite twinning mechanism is more preferable than the transformation induced plasticity (TRIP) mechanism during the early stages of deformation for a microstructure containing 15% polygonal ferrite, while the transformation induced plasticity effect is the main mechanism when there is 50% of polygonal ferrite in the microstructure. The bainitic ferrite morphology affects the deformation mode of retained austenite during straining. The polygonal ferrite behaviour during straining depends on dislocation substructure formed due to the deformation and the additional mobile dislocations caused by the TRIP effect. Operation of TRIP or twinning mechanisms depends not only on the chemical and mechanical stability of retained austenite, but also on the interaction of the phases during straining.

KEYWORDS: Transformation induced plasticity steel, thermomechanical processing, retained austenite, TRIP/TWIP effects, transmission electron microscopy, atom probe tomography

INTRODUCTION

The demand for high strength and high formability steels has recently increased. These steels have found application in the manufacture of automotive wheels, certain brackets and, potentially, of high strength drawn bars. Multiphase steels, containing austenite and bainite, represent a new class of steel with improved strength-ductility balance. The Transformation Induced Plasticity (TRIP) effect has been widely cited to be solely responsible for this balance [1, 2]. However, mechanical twinning can also occur in a steel alloyed with manganese, silicon and aluminium [3, 4]. This could lead to an increase in plasticity through the Twinning Induced Plasticity (TWIP) effect. The main aim of previous investigations has been to obtain the maximum amount of stable retained austenite [5, 6]. However, the current state of knowledge regarding the multiphase steels has revealed certain contradictions to this concept. Firstly, the distribution of carbon within the retained austenite crystals is inhomogeneous and depends on the position of these crystals in the multiphase structure. This leads to the formation of retained austenite crystals with different carbon content [7]. It has been suggested that only the retained austenite with an optimum carbon content can provide the TRIP/TWIP effect and improve the elongation [8]. Furthermore, an increase in the volume fraction of the retained austenite leads to a decrease in the average carbon of this phase, thereby reducing its chemical stability. Hence, the optimum volume fraction of the retained austenite is needed to provide the TRIP/TWIP effect [8].

The size of the retained austenite also affects the stability. Coarse retained austenite blocks have lower stability than films, for example, and tend to transform to martensite at low strain. Hence, retained austenite only with optimum size can provide the TRIP effect [6]. It has been suggested [9, 10] that there is another mechanism responsible for the unique strength-ductility balance in multiphase steels in addition to the TRIP/TWIP effects. Recent publications have revealed the importance of the effect of all phases formed in the microstructure and their interaction during straining [9, 10].

A multiphase microstructure has usually been generated by a two stage intercritical annealing due to the sensitivity of the microstructure to the thermomechanical processing approach. In the current approach, however, thermomechanical processing was used to avoid the extra step required by the intercritical annealing and develop the desirable microstructure directly after hot rolling.

The aim of the current research is to study the effect of the volume fraction of the phases on the structure-property relationship and the complex interrelationship between the phases during the formation of the final microstructure.

EXPERIMENTAL PROCEDURE

Steel with composition of Fe-0.2C-1.5Mn-1.2Si-0.3Mo-0.6Al-0.02Nb (wt%) was studied. A laboratory rolling mill was used to simulate rolling. The thermomechanical processing schedule was constructed based on analysis of the continuous cooling transformation data [11], to form 15% and 50% of polygonal ferrite and non-carbide bainitic ferrite to stabilize the retained austenite at room temperature (Fig. 1).

I.B. Timokhina, P.D. Hodgson, H. Beladi
Deakin University, Australia

E.V. Pereloma
The University of Wollongong, Australia

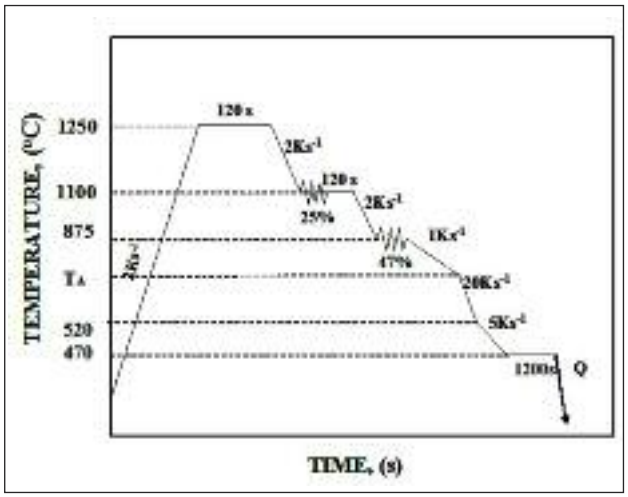

FIG. 1 ***Thermomechanical processing schedule.***
Schema del processo termomeccanico.

The samples with initial thickness of ~ 35mm were austenitized at 1250°C for 120s in a 15kW muffle furnace and then rolled at 1100°C, where the first deformation (ε_1=0.25) took place, followed by the second deformation (ε_2=0.47) at 875°C (Fig. 1). After that, the samples air cooled at ~1Ks^{-1} to the accelerated cooling start temperatures (T_A) of 780°C and 760°C to form 15% and 50% of polygonal ferrite respectively. Two spray guns were used to cool the samples at ~20Ks^{-1} to 520°C to avoid pearlite formation and after that the samples were placed in a fluidbed furnace and covered with aluminum oxide sand to hold the samples at 470°C for 1200s to form non-carbide bainite. After holding the samples were quenched in an iced brine solution (Fig. 1). The final thickness of the slab after processing was 7 mm.

The microstructure of the samples was characterized using optical metallography, transmission electron microscopy (TEM) and atom probe tomography (APT). Thin foils for TEM were prepared by twin-jet electropolishing using 5% of perchloric acid in methanol at -25°C and an operating voltage of 50V. Bright and dark-field images and selected area electron diffraction patterns were obtained using a PHILIPS CM 20 microscope operated at 200kV. The stability of retained austenite and the transformation behavior of the phases as a function of the plastic strain were studied on the samples after interrupted tensile testing using TEM.

APT analysis was performed to study the microstructural features formed after TMP, such as carbon distribution within the phases, formation of particles, etc. The standard two-stage electropolishing procedure was used to prepare the atom probe specimens [12]. The local electrode atom probe was operated at a pulse repetition rate of 200 kHz, a 20% pulse fraction with a sample temperature of 80K. Iso-concentration surfaces were used for easier visualization of the phases and carbides.

X-ray diffraction (XRD) analysis was performed using a PHILIPS PW 1130 (40kV and 25mA) diffractometer equipped with a monochromator and Cu$K\alpha$ radiation to calculate the volume fraction of retained austenite after TMP and for the samples after different strains. The integrated intensities of the $(200)_\alpha$, $(211)_\alpha$, $(200)_\gamma$ and $(220)_\gamma$ peaks were used in the direct comparison method [13].

Room-temperature mechanical properties were determined using an Instron 4500 servohydraulic tensile-testing machine with a 100kN load cell. Subsize samples with a 25mm gage length were used to minimize the amount of material.

RESULTS AND DISCUSSION

Structure-Property Relationship after TMP.

The microstructures after laboratory rolling consisted of 15±3% ferrite (hereafter called "Steel 1") and 50±4% ferrite (hereafter called "Steel 2"), with 16.5±3% and 12±3% retained austenite correspondingly and remaining non-carbide bainite and martensite. The average ferrite grain size was 2.4±0.5μm for the Steel 1 and 6.0±0.5μm for the Steel 2 (Figs. 2 a, b). The average carbon content of retained austenite measured by X-ray was 1.8wt% for Steel 1 and 1.6wt% for Steel 2.

TEM of Steel 1 revealed the formation of two bainitic morphologies: (i) granular and (ii) acicular. Granular bainite is characterized by the presence of coarse bainitic ferrite plates with isolated crystals of retained austenite in between (Figs. 3 a, b). Some of the retained austenite crystals showed twinning and the retained austenite/twinned austenite constituent islands were also present in the microstructure (Figs. 3 a, b). The acicular bainite/ferrite structure appeared to be a bainitic structure with retained austenite layers between bainitic ferrite laths (Fig. 3 c). The thickness of the bainitic laths varied from 0.1 to 0.5μm. The retained austenite laths had a wide range of thickness, from very thin retained austenite films to thick retained austenite laths, which shown in some cases twinning (Fig. 3 d). The retained austenite crystals at the polygonal ferrite/bainite interface were not observed. It is interesting to note that the clusters of bainitic ferrite laths were oriented in different directions and in some

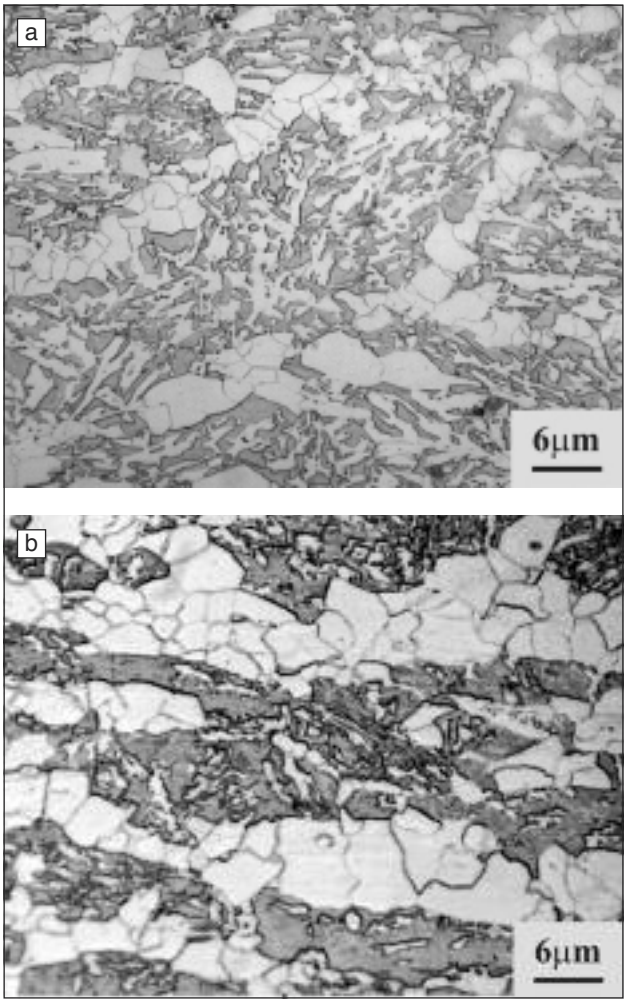

FIG. 2 ***Optical micrographs of Steel 1 (a) and Steel 2 (b).***
Micrografie ottiche di Steel 1 (a) e di Steel 2 (b).

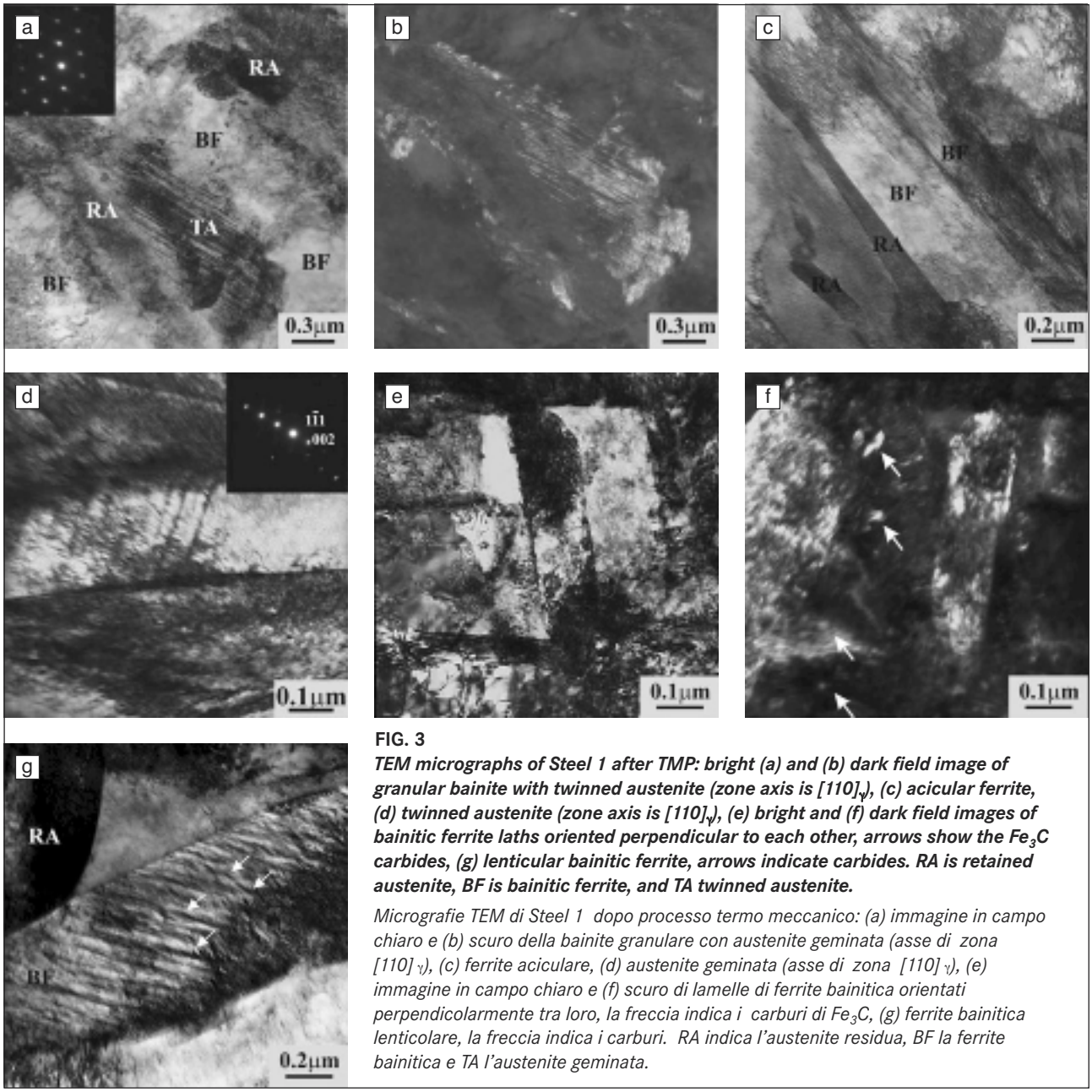

FIG. 3

TEM micrographs of Steel 1 after TMP: bright (a) and (b) dark field image of granular bainite with twinned austenite (zone axis is [110]$_\gamma$), (c) acicular ferrite, (d) twinned austenite (zone axis is [110]$_\gamma$), (e) bright and (f) dark field images of bainitic ferrite laths oriented perpendicular to each other, arrows show the Fe_3C carbides, (g) lenticular bainitic ferrite, arrows indicate carbides. RA is retained austenite, BF is bainitic ferrite, and TA twinned austenite.

Micrografie TEM di Steel 1 dopo processo termo meccanico: (a) immagine in campo chiaro e (b) scuro della bainite granulare con austenite geminata (asse di zona [110] γ), (c) ferrite aciculare, (d) austenite geminata (asse di zona [110] γ), (e) immagine in campo chiaro e (f) scuro di lamelle di ferrite bainitica orientati perpendicolarmente tra loro, la freccia indica i carburi di Fe_3C, (g) ferrite bainitica lenticolare, la freccia indica i carburi. RA indica l'austenite residua, BF la ferrite bainitica e TA l'austenite geminata.

cases perpendicular to each other (Figs. 3 e, f). Rounded Fe_3C carbides were observed within these laths (Figs. 3 f). Bainitic ferrite laths with a lenticular shape and an average thickness of 0.5μm and with fine, plate-like Fe_3C carbides were also observed in the microstructure (Fig. 3 g). Martensite crystals were not found during TEM observation.

TEM of Steel 2 also showed the formation of two types of bainite with bainitic ferrite, one in the form of parallel thin laths with an average thickness of 0.6μm and the other in the form of plates (Figs. 4 a, b). Most of the retained austenite was present as small islands, although coarse blocks of retained austenite were also found in the vicinity of the martensite (Fig. 4 b). A number of the retained austenite crystals

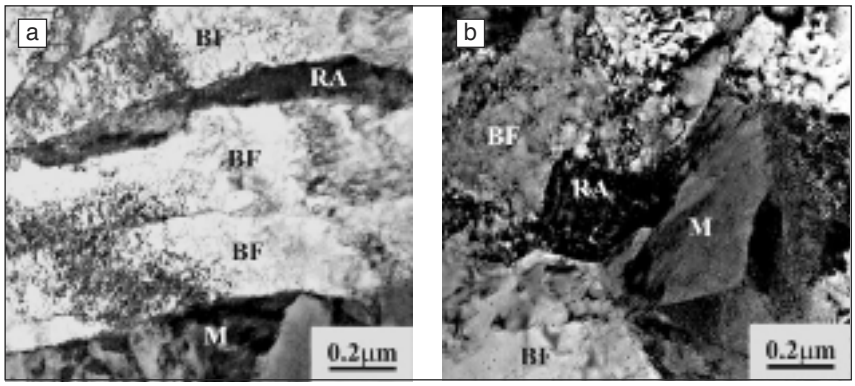

Fig. 4 ***TEM micrographs of Steel 2 after TMP: (a) acicular ferrite and (b) granular bainite. BF is bainitic ferrite, RA is retained austenite and M is martensite.***

Micrografie TEM di Steel 2 dopo processo termo meccanico: (a) ferrite aciculare e (b) bainite granulare. BF indica la ferrite bainitica, RA l'austenite residua, e M la martensite.

TAB. 1
Phase compositions calculated using APT, (at%).
Composizioni delle fasi calcolate mediante APT, (% atomico).

	Steel 1			Steel 2		
(at%)	PF	BF	RA	PF	BF	RA
C	0.04±0.02	0.4±0.2	2.4±0.7	0.02±0.001	0.25±0.03	2.71±0.07
Mn	1±0.2	1.3±0.5	1.56±0.07	0.75±0.02	1.85±0.1	1.03±0.04
Si	2.7±0.5	3.0±0.2	3.4±0.1	2.77±0.05	2.09±0.1	4.01±0.08

FIG. 5
Representative atom maps of C (a, d), Mo (b) and Nb (c) showing Nb-Mo-C carbides in retained austenite (a, b, c) and different phases in Steel 1(d). PF is polygonal ferrite, RA is retained austenite, BF is bainitic ferrite.
Mappe della distribuzione degli elementi, rappresentative di C (a, d), Mo (b) e Nb (c) che mostrano i carburi Nb-Mo-C nell' austenite residua (a, b, c) e nelle diverse fasi entro Steel 1(d). PF rappresenta la ferrite poligonale, RA l'austenite residua e BF la ferrite bainitica.

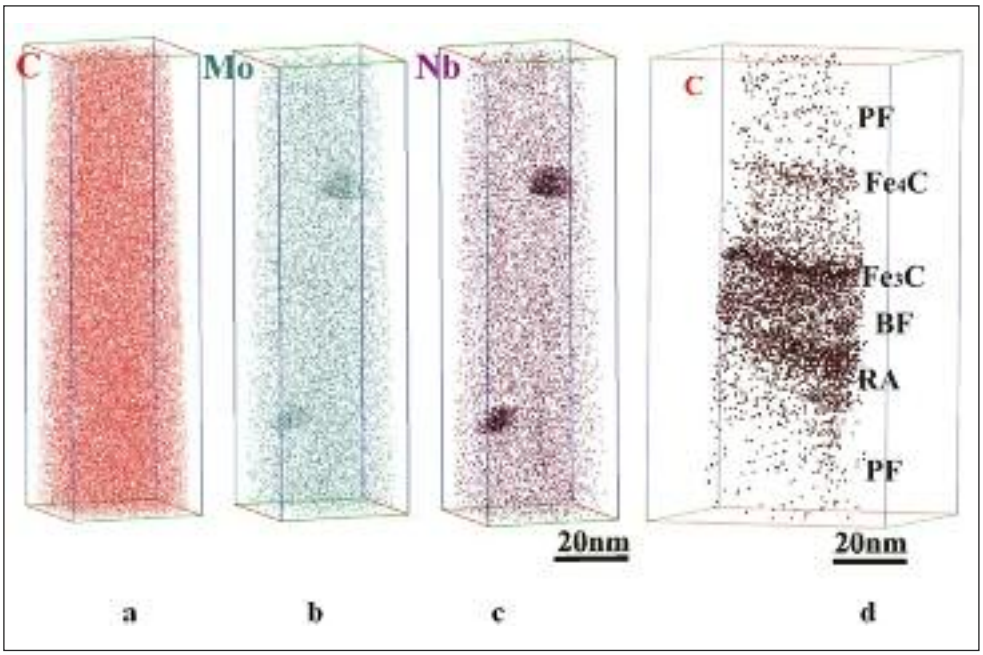

showed partial decomposition to martensite. Coarse blocks of martensite were found between the bainitic ferrite laths and at the polygonal ferrite/bainite interface. Twinned austenite was not observed by TEM in this steel.
The APT study showed formation of sphere-like Nb carbides and Nb-Mo carbides in the retained austenite and Nb carbides in the bainitic ferrite for both steels. The average size of the particles was 10±1nm (Fig. 5). The composition of phases calculated using APT is shown in Table 2. The carbon concentration in polygonal ferrite and in bainitic ferrite of Steel 1 was higher than in Steel 2 due to the difference in cooling schedules, which affected the temperature intervals for phase transformations. It leads to lower carbon content of retained austenite in Steel 1 compared to Steel 2 (Table 1). The detailed explanation of the solute distribution within the phases in Steel 2 was reported elsewhere [11]. Fe_3C and Fe_4C carbides were also observed in the microstructures of both steels using APT (Fig. 5d)
The microstructures formed after TMP control the combination of strength and ductility in the TRIP steel. While the presence of ferrite and retained austenite leads to high elongation, martensite and bainite are responsible for strength. The Steel 1 had a higher ultimate tensile strength (UTS) 1300±20MPa and yield strength (YS) 600±30MPa than Steel 2 with UTS of 1000±40MPa and YS of 400±40MPa, while the total 25±3% and uniform 17±3% elongations of Steel 1 were lower than Steel 2, with a total elongation of 29±2 and uniform elongation of 23±1% (Fig. 6). The lower elongation in the Steel 1 could be due to the lower volume fraction of polygonal ferrite. On the other hand, the higher volume fraction of retained austenite in Steel 1 should lead to higher elongation. In order to understand structure-property relationship in these steels, the behaviour of the microstructures during straining was studied using interrupted tensile tests.

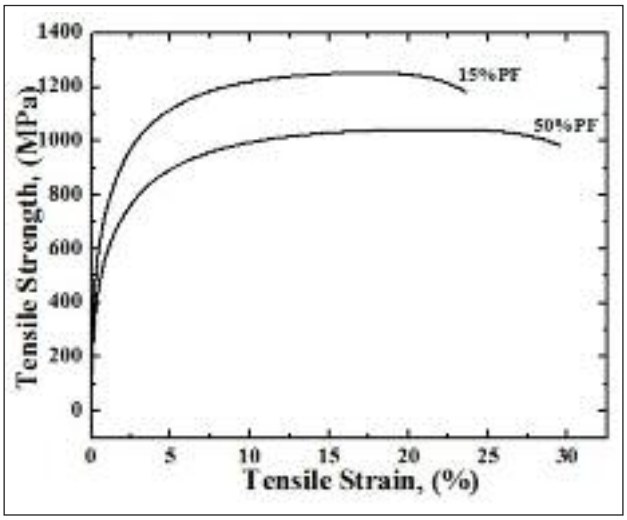

FIG. 6 ***Representative true stress-strain curves of Steel 1 and Steel 2.***
Curve rappresentative del rapporto reale carico-deformazione di Steel 1 e Steel 2.

Microstructural Behavior under Applied Strain.
X-ray analysis of Steel 1 after ~0.04 strain showed a decrease in the retained austenite volume fraction from 16.5±3% to 11±2%, which remained unchanged up to ~0.08 strain. Further decrease in the retained austenite volume fraction to 5% was observed at ~0.17 of strain. TEM revealed extensive twinning of the retained austenite crystals after a strain of 0.04 (Fig. 7a) with further development of this structure at a strain of 0.08. An increase in strain to 0.17 led to the formation of coarse marten-

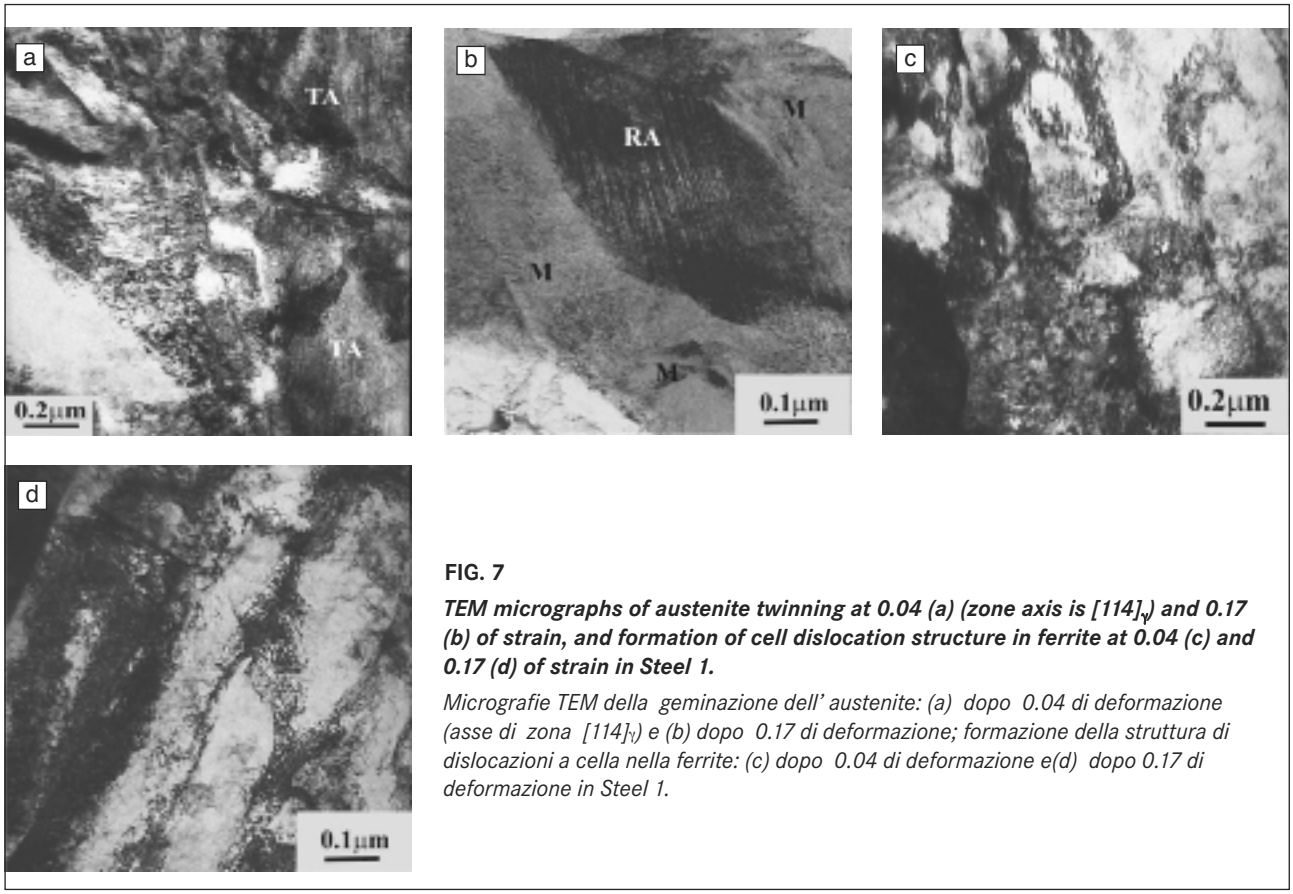

FIG. 7

TEM micrographs of austenite twinning at 0.04 (a) (zone axis is $[114]_\gamma$) and 0.17 (b) of strain, and formation of cell dislocation structure in ferrite at 0.04 (c) and 0.17 (d) of strain in Steel 1.

Micrografie TEM della geminazione dell' austenite: (a) dopo 0.04 di deformazione (asse di zona $[114]_\gamma$) e (b) dopo 0.17 di deformazione; formazione della struttura di dislocazioni a cella nella ferrite: (c) dopo 0.04 di deformazione e(d) dopo 0.17 di deformazione in Steel 1.

site crystals, although twinned austenite crystals were still observed (Fig. 7b). This suggests that austenite twinning is the preferred deformation mechanism at low strains in Steel 1. It appeared that the formation of the higher volume fraction of bainite is responsible for this behavior, i.e. during straining the bainitic ferrite laths could accommodate the stress and prevent transformation of retained austenite to martensite and, thus. promote the formation of austenite twinning at the early stages of straining.

Most of the retained austenite transformed to martensite at an intermediate strain level (0.17) due to an increase in the dislocation density of bainitic ferrite and interaction between the rigid bainitic ferrite laths and retained austenite. This leads to reduction of total elongation in Steel 1. Polygonal ferrite showed the partial formation of dislocation cells after a strain of 0.04 and parallel deformation bands after a strain of 0.17 (Figs. 7 c, d).

The transformation of the retained austenite to martensite during straining of Steel 2 occurred gradually – ~8% of retained austenite and ~12% of martensite at the ~0.08 strain; ~5% of retained austenite and ~15% of martensite at ~0.27 strain. The preferred deformation mechanism for retained austenite at all strains was TRIP effect (Figs. 8 a and b). However, ~4-5% of retained austenite was trapped between the bainitic ferrite laths and remained in the microstructure of the fractured tensile sample (Fig. 8 c).

This behavior could be explained by the combined effect of the inhomogeneous carbon distribution within the retained austenite and the effect of the size of the retained austenite on its stability. The carbon distribution within the retained austenite is not homogeneous and some coarser islands of retained austenite were less enriched than smaller ones. These coarse blocks of austenite tend to transform to martensite at a lower strain. The microstructure of Steel 2 contained a high volume of relatively coarse austenite crystals, which did not contribute significantly to the TRIP effect. On the other hand, as a result of the strain-induced transformation of high numbers of austenite blocks stress transfers to the soft ferrite matrix leading to dislocation strengthening of the neighbouring regions, which, in principal, can improve strength-ductility balance. The fine islands of austenite that are trapped between the plates of bainitic ferrite in a sheaf are much more stable because of the higher carbon concentration and also because of the physical constraint to transformation due to the close proximity of plates in all directions [14]. The contribution of their strain-induced transformation to the improved ductility is higher than the contribution of coarse crystals. On the other hand, a number of supersaturated retained austenite crystals remained in the microstructure after fracture and did not contribute to an increase in elongation.

CONCLUSIONS

The analysis of microstructure-property relationships in thermomechanically processed multiphase steels with different amounts of phases has been conducted. The results have shown that the strengthening mechanism in these complex multiphase microstructures is determined not only by the amount of retained austenite but also by the volume fraction of other phases in the microstructure and their interaction during deformation.

ACKNOWLEDGEMENTS

The authors would like to acknowledge Professor S.P. Ringer from Australian Key Centre for Microscopy and Microanalysis for providing access to the local electrode atom probe. One of the authors (PDH) acknowledges the support of the ARC Federation Fellowship scheme.

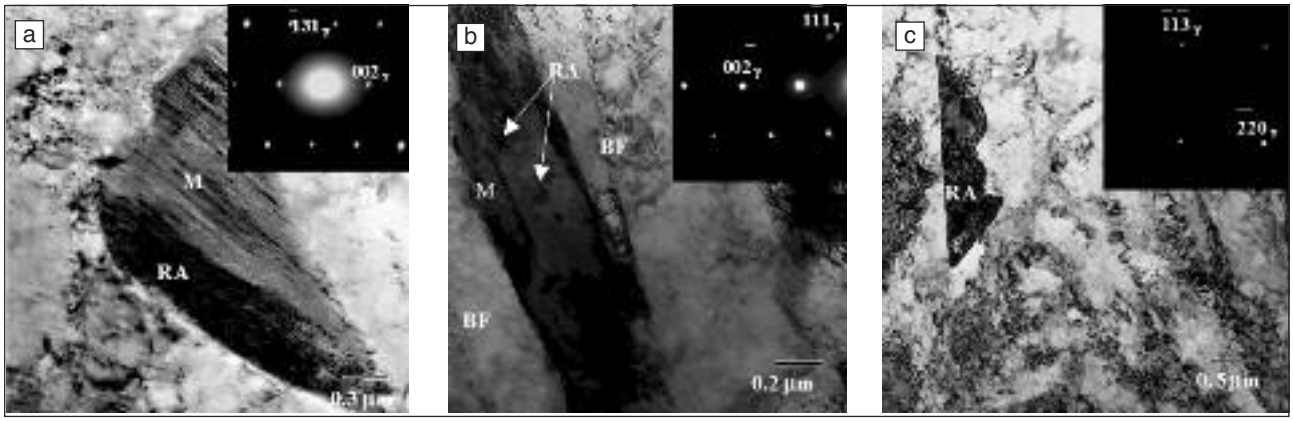

FIG. 8 ***TEM micrographs of partial transformation of retained austenite to martensite at 0.02 strain, zone axis is [310]$_\gamma$(a), partial transformation of retained austenite to martensite at 0.08 strain, zone axis is [110]$_\gamma$ (b) and retained austenite island after fracture, zone axis is [116]$_\gamma$ (c).***

Micrografie TEM della trasformazione parziale in martensite dell'austenite residua (a) dopo 0.02 di deformazione (asse di zona [310]$_\gamma$) , (b) trasformazione parziale in martensite dell'austenite residua dopo 0.08 di deformazione (asse di zona [110]$_\gamma$) e (c) isola di austenite residua dopo rottura (asse di zona [116]$_\gamma$).

REFERENCES

1. V.F. ZACKAY, E.R.PARKER, D. FAHR AND R. BUSCH: Trans. ASM, 60 (1967), p. 252.
2. W.W. GERBERICH, P.L. HEMMINGS, M.D. MERZ AND V.F. ZACKAY: Trans. Tech. Notes, 61 (1968), p. 843.
3. V. TSAKIRIS, D. V. EDMONDS: Mater. Scin. Eng, 273-275 (1999), p. 430.
4. O. GRASSEL, G. FROMMEYER, C. DERDER, H. HOFMANN: J. Phys IV France7, C5 (1997), p. 383.
5. Y. SAKUMA, O. MATSUMURA AND H. TAKECHI: Metall. and Mater. Trans. 22A (1991), p. 489.
6. D.Q. BAI, A.D. CHIRO AND S. YUE: Mater. Science Forum, Trans. Tech. Publications, Switzerland, 284-285 (1998), p. 253.
7. N.C.GOEL, S. SANGAL, K. TANGRI: Metall. And Mater. Trans., 16A (1985), p. 2013.
8. M.L. BRANDT, G.B. OLSON, Iron and Steelmaker, 20, 5(1993), p. 55.
9. I.B. TIMOKHINA, P.D. HODGSON, E.V. PERELOMA: Metall. And Mater. Trans. 35A (2004), p. 2331.
10. J. BOUQUEREL, K. VERBEKEN, B.C. De COOMAN: Acta Mater. 54 (2006), p. 1443.
11. E.V. PERELOMA, I.B. TIMOKHINA, M.K. MILLER, P.D. HODGSON: Acta Mater., 55 (2007), p. 2587.
12. M.K. MILLER, Atom Probe Tomography, in: Handbook of Microscopy for Nanotechnology, eds. N. YAO and Z.L. WANG, Kluwer Academic Press, New York (2005), p.236.
13. B.D. CULLITY, Elements of X-ray diffraction, Addison-Wesley, London (1978) p.411.
14. M. TAKAHASHI, B.K.D.H. BHADESHIA: Mater. Trans., JIM, 32(1991), p.689.

Abstract

Microstruttura e proprietà meccaniche degli acciai trip sottoposti a processi termomeccanici

Parole chiave:
acciaio, processi termomeccanici, caratterizzazione materiali

Nel presente lavoro è stato studiato il meccanismo di innalzamento delle caratteristiche meccaniche frutto della combinazione di allungamento e carico di rottura di un acciaio multifase Fe-0.2C-1.5Mn-1.2Si-0.3Mo-0.6Al-0.02Nb (% in peso). Le microstrutture con diverse frazioni in volume di ferrite poligonale, bainite e austenite residua sono state realizzate mediante trattamento termomeccanico controllato. La prova a trazione interrotta è stata utilizzata per studiare il comportamento della ferrite bainitica, dell'austenite residua e della ferrite poligonale in funzione della deformazione plastica. Per caratterizzare la frazione in volume e il contenuto di carbonio dell' austenite residua è stata utilizzata l'analisi mediante raggi X.
La microscopia elettronica a trasmissione è stata utilizzata per analizzare l'effetto della morfologia della ferrite bainitica sulla trasformazione dell' austenite residua, indotta da deformazione, e sulla geminazione dell'austenite residua sempre in funzione della deformazione nel materiale. Lo studio ha dimostrato che il meccanismo di geminazione dell'austenite è preferibile rispetto al meccanismo della plasticità indotta da trasformazione (Transformation Induced Plasticity - TRIP) durante le prime fasi di deformazione di una microstruttura contenente il 15% di ferrite poligonale, mentre l'effetto dal TRIP è il meccanismo principale quando è presente il 50 % di ferrite poligonale nella microstruttura.
La morfologia della ferrite bainitica influisce sulla modalità di deformazione dell' austenite residua durante la deformazione.
Il comportamento della ferrite poligonale durante la deformazione dipende dalla sotto-struttura delle dislocazioni dovuta alle deformazioni e dalle ulteriori dislocazioni mobili causate dall'effetto TRIP. Il verificarsi dei meccanismi di TRIP o di geminazione dipende non solo dalla stabilità chimica e meccanica dell' austenite residua, ma anche dall'interazione delle fasi durante la deformazione.